

Article

A Study of the Effect of Freeze–Thawing by Liquid Nitrogen on the Mechanical and Seepage Characteristics of Coal with Different Moisture Content Values

Xiaohan Qi ^{1,2}, Shuangrong Hou ^{1,2,*}, Heng Ma ^{1,2}, Pin Wang ^{1,2}, Yang Liu ^{1,2} and Xiaoqi Wang ^{1,2}¹ College of Safety Science and Engineering, Liaoning Technical University, Huludao 125105, China² Key Laboratory of Mine Thermodynamic Disasters and Control of Ministry of Education, Liaoning Technical University, Huludao 125105, China

* Correspondence: houshaungrong@163.com; Tel.: +86-183-4298-5963

Abstract: In order to study the effect of freezing and thawing of liquid nitrogen on the mechanical and seepage characteristics of coal rock with different water content values, conventional triaxial loading tests on freeze–thawed coal samples with different water content values were carried out using non-contact digital image processing technology. The research results showed that with the same water content, the peak strength of a liquid nitrogen freeze–thawed coal sample was smaller than that of a non-freeze–thawed coal sample, and the Poisson’s ratio was larger than that of the non-freeze–thawed coal sample; compared with the non-freeze–thawed coal sample, the strain fluctuation and concentration in the stages of compression density, elasticity, yield, and damage were weakened after freeze–thawing by liquid nitrogen, but the local stress concentration was more obvious; the non-freeze–thawed coal sample mainly showed single shear damage, and the damage fissures were inclined fissures with small openings. The higher the water content, the more obvious the tensile damage; with the increase in water content, the permeability of non-freeze–thawed coal samples showed a linear decreasing trend, and the permeability of coal samples was $0.03 \times 10^{-3} \mu\text{m}^2$ when the water content reached 9%. The permeability of freeze–thawed coal samples showed a non-linear increasing trend, and the higher the water content under the effect of expansion, the faster the permeability growth rate; the permeability of coal samples could reach $6.30 \times 10^{-3} \mu\text{m}^2$ when the water content was 9%. The results of the study can provide a theoretical guidance for gas permeation enhancement in deep low-permeability coal seams.



Citation: Qi, X.; Hou, S.; Ma, H.; Wang, P.; Liu, Y.; Wang, X. A Study of the Effect of Freeze–Thawing by Liquid Nitrogen on the Mechanical and Seepage Characteristics of Coal with Different Moisture Content

Values. *Processes* **2023**, *11*, 1822.<https://doi.org/10.3390/pr11061822>

pr11061822

Received: 28 May 2023

Revised: 9 June 2023

Accepted: 14 June 2023

Published: 15 June 2023



Copyright: © 2023 by the authors. Licensee MDPI, Basel, Switzerland. This article is an open access article distributed under the terms and conditions of the Creative Commons Attribution (CC BY) license (<https://creativecommons.org/licenses/by/4.0/>).

Keywords: mechanical; seepage; coal; water content; gas permeation; deep low permeability; coal seams

1. Introduction

In the context of increasingly limited fossil energy reserves and environmental pollution, coalbed methane (CBM) as an unconventional natural gas resource with rich reserves is increasingly valued [1]; however, with increasing mining depth, the permeability of coal rock where CBM is stored gradually decreases, and the existing permeability enhancement techniques such as hydraulic fracturing, deep hole blasting, and intensive borehole extraction in deep CBM in mining can cause water locking and water sensitivity [2,3]. In recent years, liquid carbon dioxide, liquid nitrogen, and other low-temperature fluids have been gradually applied to coalbed methane penetration mining [4]. Liquid nitrogen freeze–thaw penetration augmentation has the advantages of not polluting the reservoir, no hydration expansion, and high efficiency [5], and gasified nitrogen during penetration augmentation can reduce the partial pressure of methane gas in the coal seam, accelerate the resolution of coalbed methane, and improve the extraction rate of coalbed methane [6,7]. Therefore, it is necessary to further study the influence and laws of liquid nitrogen on the mechanical and percolation characteristics of coal samples with different water content values.

The mechanical and seepage properties of raw coal change due to hydrolock softening and other effects of groundwater on underground coal rocks. In a study of water content on the mechanical and seepage characteristics of coal rock, Wang Shukun et al. [8] examined the effect of water on the strength and deformation characteristics of coal rock and concluded that the compressive strength and elastic energy index of coal rock decreased with the increase in water content. Cheng Qiaoyun [9] conducted experiments on the evolution of the permeability of coal rock with different water content values and established a model of permeability under the synergistic effect of effective stress and intrinsic water based on the thickness of the water film in matrix pores and fractures. Chang Yanan [10] conducted uniaxial compression and acoustic emission tests on specimens with different water content values and found that mechanical parameters such as compressive strength, elastic modulus, and hardness of the specimens showed an inverse relationship with water content.

In a study of cracking patterns of coal samples by liquid nitrogen and different water content values, Shaoran Ren et al. [11] conducted cold shock tests on different coal species in both dry and water-filled states and concluded that the ultra-low temperature of liquid nitrogen and the natural water in coal rock caused freezing and expansion, resulting in the generation of thermal stress cracks and local cracks and increasing the permeability of coal rock. Ren Yongjie et al. [12] conducted CT scan tests before and after liquid nitrogen immersion in coal rock and found that the contraction–freeze expansion stress effect after liquid nitrogen immersion led to the generation of new fractures, and the new fractures interpenetrated with the original fractures in coal rock, which improved the permeability of coal rock. Wang Hao [13] carried out experiments on the effect of different liquid nitrogen treatment times and surrounding pressures on the triaxial mechanical percolation of coal samples and concluded that with the increase in liquid nitrogen treatment time, the compressive strength of coal samples first decreased and then increased until it stabilized, and the permeability increased from the initial value at an average rate of 29.84%. Coetsee Sansh et al. [14,15] carried out fracturing experiments on coal rock with liquid nitrogen freeze–thawing and found that the effect of liquid nitrogen cold immersion on the new development extension of fractures was obvious compared to direct fracturing experiments. Li Bo et al. [16] carried out a study on the mechanism of action of liquid nitrogen on water-bearing coal rocks and concluded that the permeability of coal samples increased exponentially with increasing water content after cold leaching with liquid nitrogen.

In summary, scholars have studied the mechanics and percolation laws of coal rocks with different water content values quite extensively, but there are fewer studies on the mechanics and percolation laws of liquid nitrogen on coal rocks, especially on the mechanics and percolation laws of liquid nitrogen on coal rocks with different water content values. Most research has focused on the study of liquid nitrogen on dry and water-saturated coal rocks, which differs from the actual coal rock storage environment in wells. The results of this study are of great significance in order to improve the efficiency of gas extraction and safe production in low-permeability coal seams.

2. Experimental Protocol Design

2.1. Experimental Equipment

The experimental equipment included a drilling core machine, a cutting machine, a double-end face-smoothing machine, an electric blast dryer, an HC-U7 series non-metallic ultrasonic detector, a vacuum pump, an HC-SPT-100 type high-pressure triaxial testing machine, and other instruments.

Before the experiment, the standard specimens were prepared by a drilling and coring machine, a cutting machine, and a double-ended grinding machine; the prepared standard specimens were tested by an ultrasonic detector for wave velocities; and the specimens with stable and similar wave velocities were selected and put into the electric blast drying oven and dried at 100 °C for more than 24 h. The dry mass of the specimens was recorded when the change of mass per hour did not exceed 0.2%. After drying, the specimens

were treated with vacuum pumping, and when the quality of the specimens was basically unchanged, drying was considered to be completed. The quality change curve of partially filled specimens is shown in Figure 1.

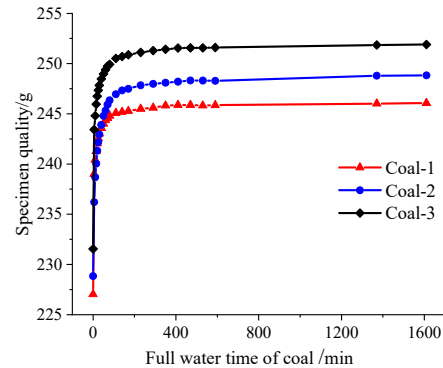


Figure 1. Specimen saturation curve.

After the water-filled specimens were naturally dried at room temperature to the preset moisture content values (3%, 6%, 9%), the specimens were subjected to liquid nitrogen freeze–thaw treatments. The coal samples with different moisture content values were loaded into insulated containers with liquid nitrogen, soaked for 10 min, and then maintained at room temperature to undergo natural thawing for 2 h. This freeze–thaw operation was then repeated, that is, each specimen was subjected to two liquid nitrogen freeze–thaw treatments. Finally, the pretreatment-completed specimens were placed in a triaxial pressure chamber after the graphical measurement of selected parameters in order to start the experiment; the experimental system is shown in Figure 2.



Figure 2. Experimental system diagram.

2.2. Experimental Protocol

In order to study the mechanical and seepage characteristics of coal seam gas extraction under different pretreatment conditions, a triaxial servo–fluid–solid coupling test system with full surface deformation measurement technology was used to carry out the loading test of liquid nitrogen on the mechanical properties and seepage of coal rock with different water content values; the test loading path is shown in Figure 3, the blue column in the figure is the stage of restoring the original stress of the coal rock, and the pink column is the loading stage after restoring the original stress of the coal rock. The working face coal depth of Wangzhuang coal mine 9101 (known as the Wangzhuang Coal Mine of Shanxi Lu’an Environmental Protection Energy Development Company Limited, located in Luzhou District, Changzhi, China) is about 420 m; the actual measurement of its maximum main

stress is 9.83 MPa, the angle with the horizontal direction is less than 7° , the vertical main stress is 8.30 MPa, and the horizontal and vertical stress ratio is 1.18. The coal samples used in the experiment were taken from the working face of Wangzhuang coal mine 9105, which has a coal seam depth of about 400 m. The ground stress of the 9105 working face was designed with reference to the actual measured values of the horizontal and vertical ground stress of the 9101 working face; the ratio of the horizontal to vertical stress of the 9101 working face is 1.18, so the simplified measure of vertical and horizontal ground stress of the 9105 working face is 9 MPa.

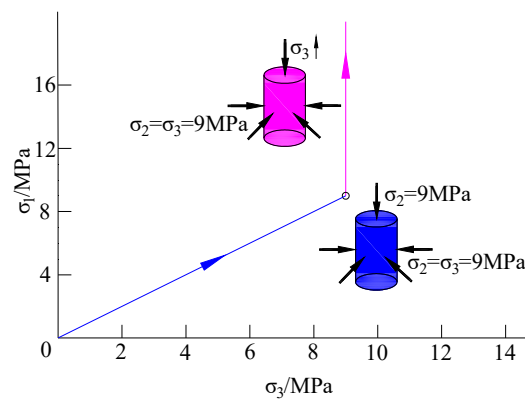


Figure 3. Schematic diagram of the experimental path.

Two sets of comparative experiments were conducted: one for conventional triaxial loading of coal samples with different moisture content values without liquid nitrogen freeze–thaw, and the other for conventional triaxial loading of coal samples with different moisture content values after two cycles of liquid nitrogen freeze–thaw.

The highest moisture content of the coal samples was 8.94% after being filled with water via vacuum pump in order to investigate the effect of liquid nitrogen on the mechanics and percolation law of coal seams with different moisture content values. The experimental coal samples were designed to have moisture content values of 0%, 3%, 6%, and 9%. However, due to the uncontrolled nature of natural air drying, the actual experimental moisture content values of the coal samples had small deviations from the preset experimental values, but for the convenience of comparative analysis, the analysis was performed according to the preset moisture content values in the subsequent analysis of the experimental results. The specimen base parameters are shown in Table 1.

Table 1. Basic coal sample parameters.

Coal Sample Number	Water Content (%)	Freeze–Thaw Times	Wave Speed (μ s)	Original Quality (g)	Quality after Treatment (g)	Height (mm)	Diameter (mm)
AJ-1	0	2	1.58	229.31	228.56	101.42	48.24
AC-2	3.05	2	1.54	228.84	235.82	100.11	49.82
AC-3	6.13	2	1.59	231.55	245.74	100.18	50.59
AC-1	8.94	2	1.53	227.03	247.33	99.82	50.11
F-2	0	0	1.77	233.42	233.42	100.09	51.04
AI-2	2.95	0	1.75	234.47	241.39	101.17	50.95
AK-3	6.01	0	1.72	233.98	248.04	99.98	50.91
AJ-3	8.89	0	1.74	232.91	253.62	100.38	49.32

2.3. Image Measurement Principal Analysis

Traditionally, strain gauges are applied to coal rock specimens or extensometers are used to measure the degree of deformation of the specimen during loading, while the

specimen body strain cannot be measured directly. The body strain is commonly calculated by the following formula:

$$\varepsilon_v = \varepsilon_v^{nb} + \varepsilon_v^b + \frac{\alpha}{K_0} p \quad (1)$$

where ε_v is the body strain; ε_v^{nb} is the non-laminated body strain; ε_v^b is the laminated body strain; α is the effective stress factor; K_0 is the bulk modulus of coal in MPa; p is the pore pressure in MPa.

Parameters ε_v^{nb} and ε_v^b are calculated as follows:

$$\varepsilon_v^{nb} = \frac{1}{E_{//1}} [\sigma_{//1} - v(\sigma_{//1} + \sigma_{\perp})] + \frac{1}{E_{//2}} [\sigma_{//2} - v(\sigma_{//2} + \sigma_{\perp})] + (1-f) \frac{1}{E_{\perp}^{nb}} [\sigma_{//\perp} - v(\sigma_{//1} + \sigma_{//2})] \quad (2)$$

$$\varepsilon_v^b = \frac{f}{3} \left[1 - \exp\left(-\frac{\sigma_{\perp}}{E_{\perp}^b}\right) \right] \quad (3)$$

where $E_{//1}$, $E_{//2}$ are the parallel laminated modulus of elasticity in MPa; E_{\perp}^{nb} , E_{\perp}^b are the non-laminated equivalent modulus of elasticity and laminated equivalent modulus of elasticity of vertical laminations, respectively, in MPa; $\sigma_{//1}$, $\sigma_{//2}$ are the parallel laminar stress in MPa; σ_{\perp} is the vertical laminar stress in MPa; v is Poisson's ratio; f is the laminar coefficient.

To calculate the body strain using axial and radial strains, the following equation is used:

$$\varepsilon_v = \varepsilon_1 + 2\varepsilon_3 \quad (4)$$

where ε_1 is the specimen axial strain in %; ε_3 is the specimen radial strain in %.

Equations (1) and (4) are used to calculate the volumetric strain of the specimen during the loading process with the help of conventional measured strains or stresses derived from the calculation, which cannot directly measure the volume change of the specimen during the loading process in real time. The digital image processing technology used in this experiment is a non-contact, non-interference deformation measurement technique for the specimen, which can reflect the local and overall deformation of the specimen simultaneously and improve the accuracy of the strain values of the axis, diameter, and body.

3. Mechanical Experimental Results and Analysis

The triaxial mechanical property curves of the specimens under different treatments are shown in Figure 4. Figure 4a shows the conventional triaxial loading curve of coal samples with different moisture content values without liquid nitrogen freeze–thawing, and Figure 4b shows the conventional triaxial loading curve of coal samples with different moisture content values after two cycles of freeze–thawing by liquid nitrogen. Among them, ε_1 , ε_3 , ε_v are the axial, radial, and bulk stress–strain curves, respectively.

The mechanical parameters of the specimens under the two groups of comparison experiments are shown in Figure 5. Under the condition of freeze–thaw treatment without liquid nitrogen, the peak strength and elastic modulus of coal samples showed nonlinear decreasing trends, and Poisson's ratio and axial peak strain showed nonlinear increasing trends with the increase in water content. The higher the water content, the more obvious the lubrication and weakening effect, resulting in the decrease in strength and modulus of elasticity with the increase in water content, and the increase in Poisson's ratio and axial peak strain with the increase in water content. For example, the decrease in peak strength values of 0–3%, 3–6%, and 6–9% of water content values were 4.83%, 5.53%, and 12.96%, respectively, and the decrease in peak strength values of 6–9% of water content were 2.66 times those between 0 and 3%.

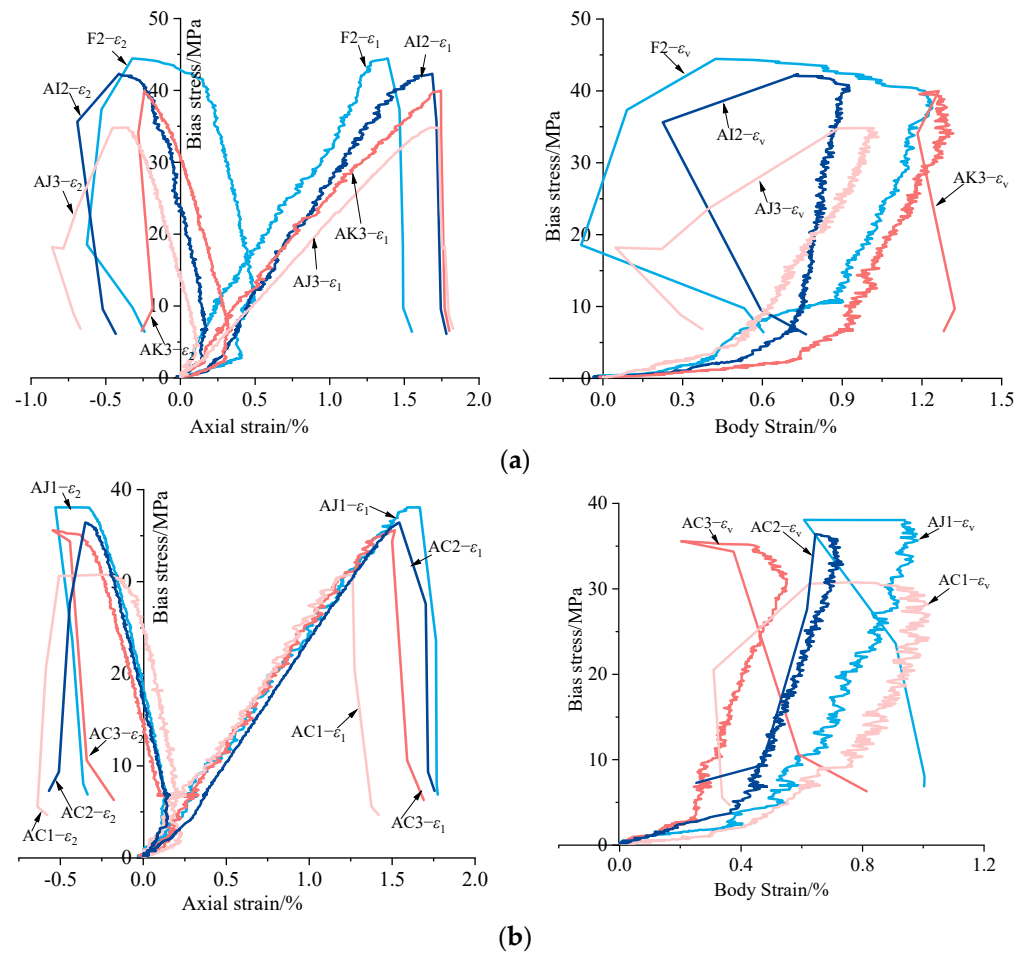


Figure 4. Triaxial mechanical properties of specimens with different treatments. (a) Coal samples with different moisture content values without liquid nitrogen freeze–thaw treatment. (b) Freeze–thaw treatment of coal samples with different moisture content values by liquid nitrogen.

After two freeze–thaw treatments with liquid nitrogen, the peak strength and axial peak strain of coal samples showed nonlinear decreasing trends, the modulus of elasticity showed an increasing and then decreasing trend, and Poisson’s ratio showed an increasing trend with the increase in water content. After liquid nitrogen was injected into the coal seam, the pore water in the primary pore fissures of the coal rock froze, and the low boiling point liquid nitrogen sublimated, both of which produced expansions in volume, and different particles of the coal rock body had different sensitivities to low temperature. The higher the water content, the more intense the water freezing and expansion, and the more significant the destruction of the coal rock structure, resulting in the decrease in coal rock strength with the increase in water content, and the increase in Poisson’s ratio with the increase in water content; due to the destruction of the coal rock structure caused by liquid nitrogen, the number of pores and fissures that could be assigned after the melting of water freezing in unit volume increased, i.e., the free water in the original pores and fissures decreased, which showed that its lubricating effect in the discontinuous boundary surface was weakened. Therefore, the axial peak strain decreased with the increase in water content.

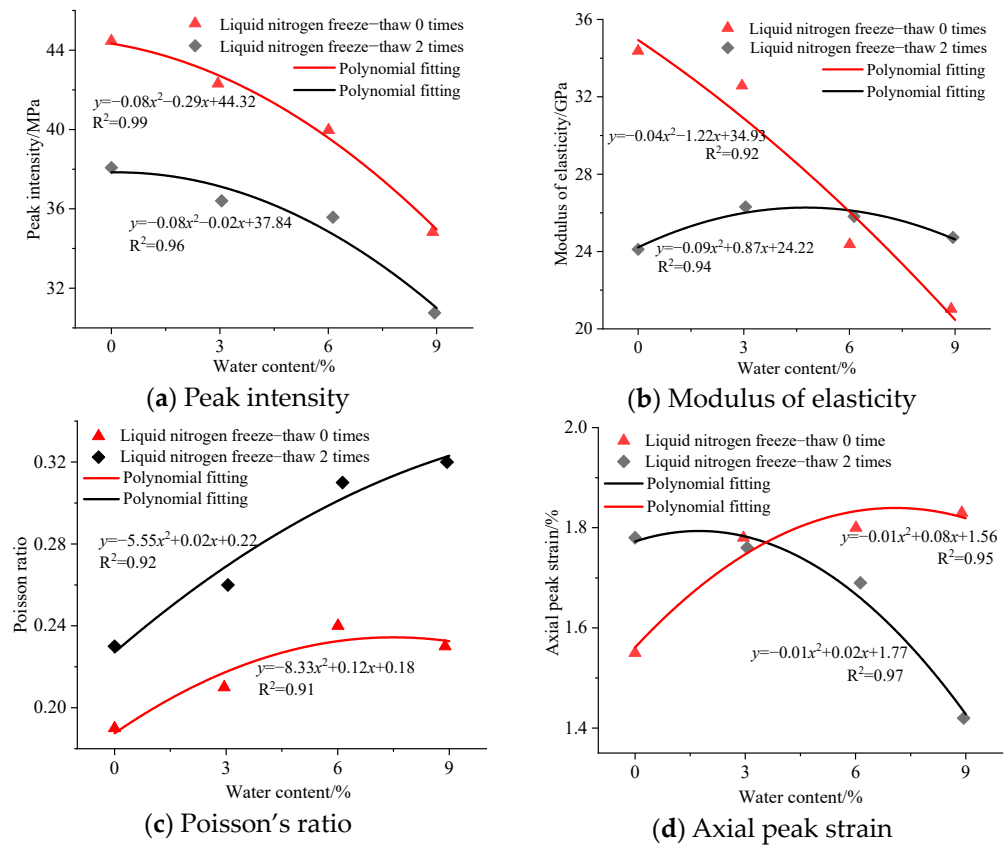


Figure 5. Specimen base mechanical parameters.

Compared with the non-freeze–thawed coal samples, the internal structural damage of coal rock was obvious after two cycles of freeze–thawing by liquid nitrogen, which showed that the peak strength of liquid nitrogen freeze–thawed coal samples was smaller than that of non-freeze–thawed coal samples, and Poisson's ratio was larger than that of non-freeze–thawed coal samples with the same water content values. The peak strength values of the non-freeze–thawed coal samples were 44.46 MPa, 42.31 MPa, 39.37 MPa, and 34.83 MPa at 0%, 3%, 6%, and 9% water content values, respectively, and the peak strength values of the coal samples after freeze–thawing with liquid nitrogen were 38.03 MPa, 36.41 MPa, 35.58 MPa, and 30.76 MPa, respectively, with decreases of 14.35%, 13.94%, and 10.98%, respectively. In combination with the significant increases in Poisson's ratio between freeze–thawed and non-frozen coal samples with 6% and 9% of water content compared with 0% and 3% of water content, it is clear that the lateral deformation capacity of coal rock was significantly enhanced after freeze–thawing using liquid nitrogen with high water content values, i.e., the internal structural damage of coal rock was more obvious. The elastic modulus was smaller than that of non-freeze–thawed coal samples at low water content values and larger than that of non-freeze–thawed coal samples at high water content. The axial peak strain was larger than that of non-freeze–thawed coal samples with low water content values and smaller than that of frozen–thawed coal samples with high water content values. The reason for the analysis is that the experimental perimeter pressure was 9 MPa, the perimeter pressure was larger, and the binding force on the ring of the specimen was strong. Then, the axial force at the time of crushing of the required axial loading was larger, and when the specimen with high water content values encountered larger axial forces, the lubricating effect of water on the boundary of discontinuous surfaces was more significant, such as fissures and joints of the coal body, i.e., less stress was required to produce unit elastic deformation, thus showing that the elastic modulus was larger than that of non-freeze–thawed coal samples with high water content values.

4. Analysis of the Strain Field and Damage Characteristics of Coal Samples at Different Stages of Loading

4.1. Strain Field Analysis of Specimen Bodies with Different Moisture Content Values

A high-pressure triaxial meter uses non-contact digital image processing technology to record the deformation of the specimen based on changes in the position of 192 corner points in six rows and eight columns of 48 squares within the selected frame diagram wrapped around the periphery of the specimen, which has high measurement accuracy and large information processing capacity and can continuously measure the full surface deformation of the specimen and the local point strain fields, such as radial strain, axial strain, shear strain, and body strain over time, overcoming the inaccuracy of deformation measurement by conventional strain gauges or using extensometers [17–22]. To further investigate the damage mechanism of liquid nitrogen freeze–thaw and moisture content on the coal samples during loading, the body strain fields of the four stages of compression, namely, density, flexibility, yield, and sabotage, during loading were plotted, as shown in Figures 6 and 7, where stress concentrations occurred in the specimens during loading under both liquid nitrogen freeze–thaw and non-freeze–thaw conditions. The part circled by red and yellow dashed lines represents the stress concentration phenomenon during the stressing process of coal rock and the damage of the specimen along the stress concentration point.

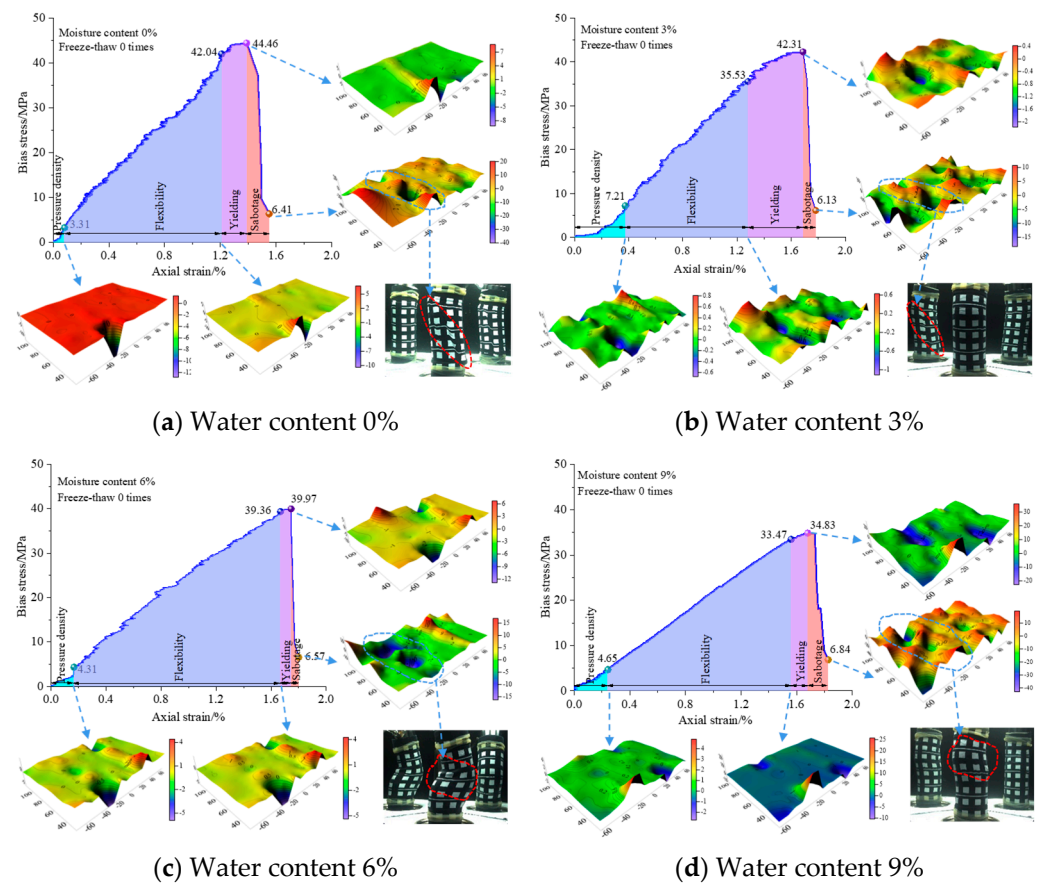


Figure 6. Four-stage body strain field of non-freeze–thawed coal samples with different water content values.

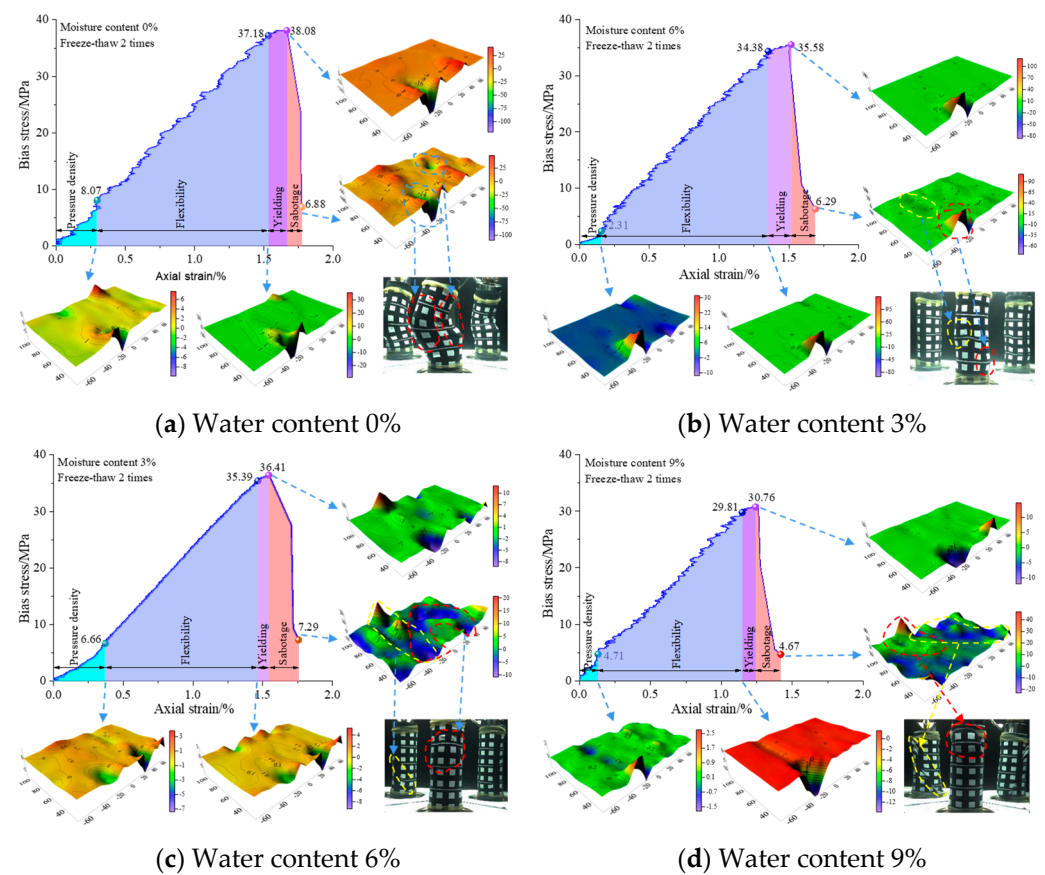


Figure 7. Four-stage body strain field of freeze–thaw coal samples with different water content values.

Under the condition of freeze–thaw treatment without liquid nitrogen, the body strain of the specimens without water showed local stress concentration in the compressive stage, the flexural and yielding stages inherited the stress concentration of the evolving body strain in the compressive stage, and the specimens in the damage stage broke through the stress concentration along the compressive stage. After the specimens acquired water, the overall fluctuation of the body strain in the compressive stage and the stress concentration phenomenon increased significantly, the elastic yielding stage inherited the stress concentration and fluctuation of the evolving body strain in the compressive stage, and the specimen in the damage stage broke along the maximum stress concentration point in the compressive stage. With the increase in water content, the overall trend of strain fluctuation and concentration in the three stages of compression, flexibility, and yielding was weakened, but the local stress concentration phenomenon was more obvious. In the yielding stage, for example, the maximum value of the body strain–stress concentration at 3% water content was -2% (negative strain value represents compression of the specimen, positive represents expansion of the specimen), and the overall fluctuation value was about -0.4% at 6% and 9% water content, the maximum value of body strain. When the moisture content was 6% and 9%, the maximum value of strain–stress concentration was -12% and 30% , respectively, and the overall fluctuation value was -1% and -3% , respectively.

After freeze–thaw treatment with liquid nitrogen, the specimens showed local stress concentrations in the compressive stage, and the elastic and yielding stages inherited the stress concentrations of evolving body strain in the compressive stage. The specimens in the damage stage broke through the stress concentrations along the compressive stage, and the stress concentrations in the 0%, 3%, and 6% damage stages were all inherited extensions of the stress concentrations in the compressive stage, except for the new stress concentrations in the 9% moisture content damage stage.

Compared with the non-freeze–thawed coal samples, the strain fluctuations and concentrations in the stages of compression, flexibility, yielding, and destruction of coal rocks after freeze–thawing with liquid nitrogen showed an overall weakening trend, but the local stress concentrations were more obvious. For example, under the condition of 6% water content, the non-freeze–thawed coal samples had about five stress concentrations in each stage of loading, but after freeze–thawing with liquid nitrogen, there was only one stress concentration in each stage of loading, but the peak body strain at the stress concentration point was much higher than the corresponding stage of non-freeze–thawed coal samples. The peak body strain at the stress concentration point was much higher than the body strain value at the corresponding stage of the non-freeze–thawed coal sample. The reason for the analysis is that after the non-freeze–thawed coal rock was treated with water, the water entered the internal pores and fissures of the coal rock to produce lubrication in the joint fault surface, resulting in the stress concentration at the end points of the fissures in the loading process, as shown in Figure 8a. After the freeze–thaw treatment of the water-bearing coal sample with liquid nitrogen, the primary fissures were extended, new fissures were created, and the intersection of the primary and new fissures formed a fissure network. The coal rock structure inside the fissure network was more seriously damaged than the coal rock structure around the other fissures, and the stress concentration was generated at the intersection of the fissures with the largest number of branches in the fissure network when subjected to an external load. The concentration phenomenon was much more obvious than that at the end points of the old and new fissures, which showed that the local stress concentration phenomenon was significantly enhanced at each stage after freezing and thawing by liquid nitrogen, resulting in a weakening trend of the overall strain fluctuation and concentration phenomenon, as shown in Figure 8b.

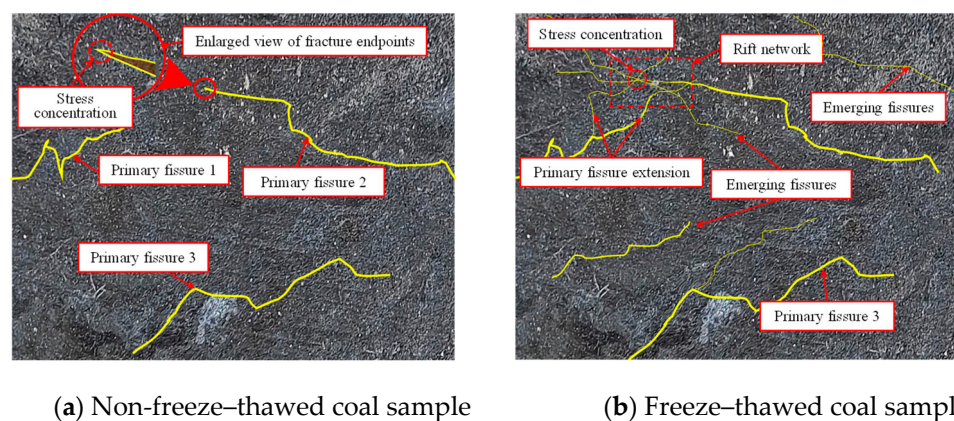
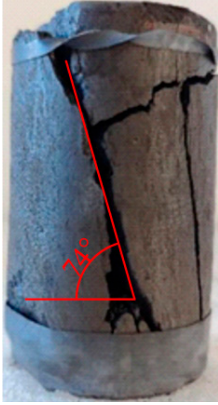


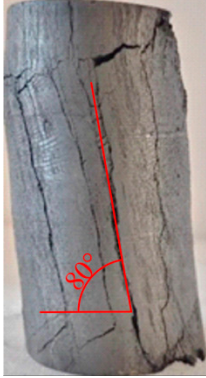

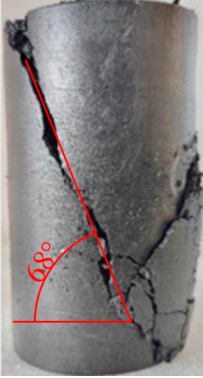
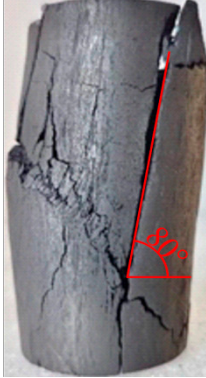



Figure 8. Schematic diagram of fracture evolution before and after freezing and thawing of coal samples.

4.2. Analysis of Damage Characteristics of Coal Samples

The coal samples after destruction under triaxial loading are shown in Table 2. The coal samples without liquid nitrogen freeze–thawing mainly showed single shear damage [23–25], and the destruction fissures were dominated by inclined fissures with small openness (except for the moisture content of 0%); the higher the moisture content, the larger the fissure inclination. Under the condition of 0% water content, the damage cracks were mainly 74° inclined with larger openness, accompanied by one inclined crack with a larger inclination angle and smaller openness. Under the conditions of 3% and 6% water content, the damage cracks were mainly inclined cracks concentrated in the lower position of the middle of the specimen, and the number of frontal cracks reached five and six, respectively, and the angle of cracks increased gradually with the increase in water content from 65° at 3% water content to 65° at 6% water content. The angle increased to 78° when the water content was 6%. With 9% water content, the damage fissures were mainly close to the test piece of inclined fissures. The number of frontal fissures decreased to four, but the fissure angle still showed a growing trend, with the main fissure dip angle of 80°.

Table 2. Crushed coal sample statistics.

Moisture Content 0%	Moisture Content 3%	Moisture Content 6%	Moisture Content 9%
Liquid Nitrogen Freeze-Thaw 0 Times			
AJ-1	AC-3	AC-1	AC-2
			
Liquid Nitrogen Freeze-Thaw 2 Times			
F-2	AI-2	AK-3	AJ-3
			

The damage fissures of liquid nitrogen freeze–thaw coal samples under the condition of no water content were similar to the damage fissures of 3%, 6%, and 9% of the coal samples without liquid nitrogen freeze–thawing, which were also mainly inclined fissures with small openness, but the damaged specimens were a combination of blocks and powder. The damage fissures were mainly inclined fissures with large openness under the conjugate damage of 3% and 6% of water content. The damage fissures were mainly inclined fissures and circumferential fissures with large openness under the tension shear damage of 9% of water content, and there were more circumferential fissures, among which there were three circumferential fissures with large openness and two circumferential fissures with small openness.

It can be seen that after the coal samples were treated with water and liquid nitrogen freeze–thawing under conventional triaxial loading, all the specimens showed shear damage except for the coal samples with 9% water content and liquid nitrogen freeze–thawing, which showed tension shear damage. The higher the water content was, the more the aqueous solution filled in the small joints and faults parallel to the axial direction, and the greater the chance of specimen slippage along the axial load parallel to the axial force when loaded under the same circumferential pressure. The fracture angle increased gradually with the increase in water content. After the freeze–thawing treatment of water-bearing coal samples with liquid nitrogen, the primary fracture extension and the new fracture generation formed a fracture network. The structural damage of coal rock in the fracture

network was much higher than that of coal rock around other primary new fractures, and the stress concentration was generated in the fracture network when subjected to external loads and caused the specimen to be damaged along the stress concentration. The number of tilted fractures after damage was much smaller than that of non-freeze–thawed coal samples.

5. Analysis of Seepage Flow Patterns before and after Freezing and Thawing of Coal with Different Moisture Content Values in Liquid Nitrogen

5.1. Analysis of Permeability before and after Freeze–Thaw

A coal body is a porous medium material, and the large amount of gases generated during the biomass coal formation process that cannot escape to the atmosphere form voids of different sizes inside the coal. The decimal classification of pore size proposed by BHODB classifies pores into micropores (diameter < 10 nm), transition pores (diameter 10–100 nm), mesopores (diameter 100–1000 nm), and macropores (diameter > 1000 nm), with micropores and transition pores, also called adsorption pores, serving as the main storage space. Mesopores and macropores serve as the main flow paths for fluids and are called percolation pores [26–29], and the flow of fluids through these pore fractures is referred to as percolation. In order to recover the original stress state of the coal sample, the experiment was started by increasing the surrounding pressure to 9 MPa at a radial loading rate of 0.02 MPa/s and then adding 1 MPa of high-purity nitrogen; the axial loading test was started after the gas flow was stabilized.

As seen in Figure 9, the permeability of the non-freeze–thawed coal sample decreased linearly with the increase in water content from $0.68 \times 10^{-3} \mu\text{m}^2$ at 0% water content to $0.03 \times 10^{-3} \mu\text{m}^2$ at 9% water content. With a decrease of 95.59%, the coal sample was basically full of water at 9% water content, and the internal pores and fissures were completely filled with water solution, and there was no channel for gas circulation.

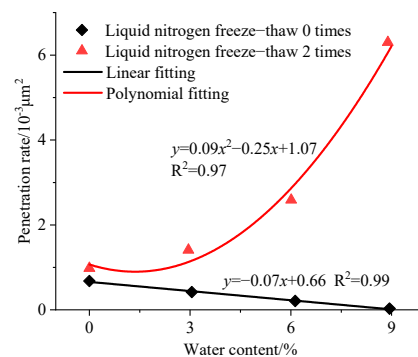


Figure 9. Initial permeability of coal samples at different water content values.

The permeability of the freeze–thawed coal samples showed a non-linear growth trend with the increase in water content, and the higher the water content, the faster the permeability growth rate. For example, the increase in permeability between 0 and 3% water content was 43.88%, the increase in permeability between 6 and 9% water content was 152.12%, and the increase in permeability between 6 and 9% water content was 3.47 times that between 0 and 3% water content. When liquid nitrogen at a temperature of $-195.8 \text{ }^\circ\text{C}$ was injected into the coal seam, the expansion force generated far exceeded the strength of the coal rock, so the higher the water content, the more the location and expansion force of the expansion generated by the freezing and thawing of liquid nitrogen inside the coal sample, the more serious the damage to the internal structure of the coal rock, and thus the greater the permeability.

5.2. Analysis of Fracture Evolution of Freeze–Thaw Coal Samples

The effect of freeze–thaw fracturing of water-bearing coal rocks by liquid nitrogen is significant, mainly relying on the expansion force generated by the phase change of water

freezing and the volume expansion of low boiling point liquid nitrogen sublimation to fracture coal rock (for the sake of space, this paper focuses on the phase change of water freezing to fracture coal rock). Because the density of liquid water is 1 g/cm^3 and that of ice is about 0.9 g/cm^3 , after solidification into ice, the mass remains the same but the density decreases, so the volume should be increased to $10/9$ of the original (about 1.11 times).

The higher the water content of fractures in coal rocks, the more obvious the volume increase after freezing by liquid nitrogen, as shown in Figure 10. When fissures without water inside the coal rock are frozen by liquid nitrogen and then thawed, there is no water solution inside the fissures to freeze and expand, and the fissures have no obvious expansion. When fissures with low water content inside the coal rock are frozen by liquid nitrogen and thawed, the fissures that have some areas of water solution accumulation expand, and the fissures with areas of water solution dispersion have no obvious expansion. When the fissures with high water content inside the coal rock are frozen by liquid nitrogen and thawed, the fissures expand as a whole.

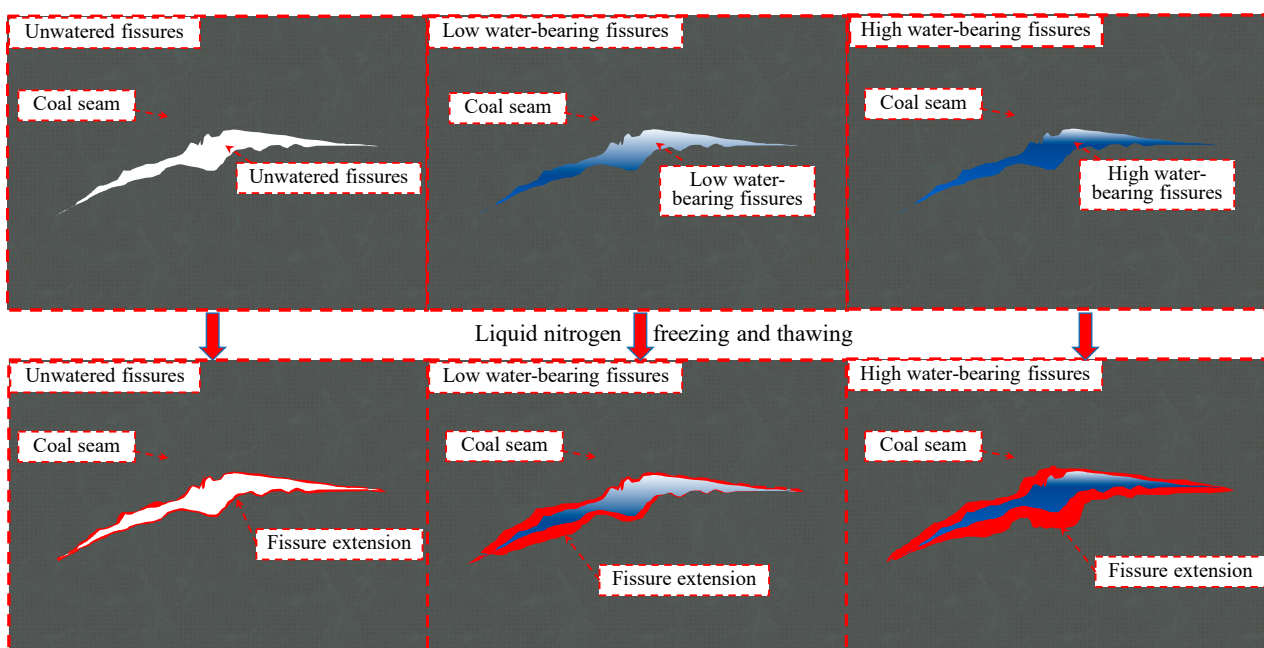


Figure 10. Freeze–thaw fracture evolution of liquid nitrogen in different water-bearing coal seams.

Underground coal rocks are mostly water-bearing coal rocks due to underground water endowment. When the adsorbed free water in the pore fissures of coal rocks encounters low-temperature liquid nitrogen, the expansion force generated by the volume increase is much larger than the linkage force between the ice and coal matrix, and the original coal pore fissures expand. When Winkler [30] performed low-temperature fracturing of water-bearing coal rocks, he found that the expansion forces generated by pore water freezing at $-5 \text{ }^\circ\text{C}$, $-10 \text{ }^\circ\text{C}$, and $-22 \text{ }^\circ\text{C}$ were 61 MPa, 113 MPa, and 211.5 MPa, respectively, which were much greater than the linkage forces between the ice and the coal matrix. With the increase in water content, the expansion and addition of fissures in coal samples after freeze–thawing with liquid nitrogen increased significantly, as shown in Figure 11. The maximum opening of fissures on the end face of the original non-freeze–thawed coal sample was 0.143 mm at 0% water content, and the maximum opening of fissures was 0.161 mm after two cycles of freeze–thawing with liquid nitrogen, with an increase of 0.018 mm or 12.59%. At 9% water content, the maximum opening of fissures on the end face of the original non-freeze–thawed coal sample was 0.014 mm, with an increase of 0.269 mm or 1921.43%. Therefore, the higher the water content, the more obvious the pore fissure expansion phenomenon is after freezing and thawing with liquid nitrogen, and therefore the greater the permeability is.

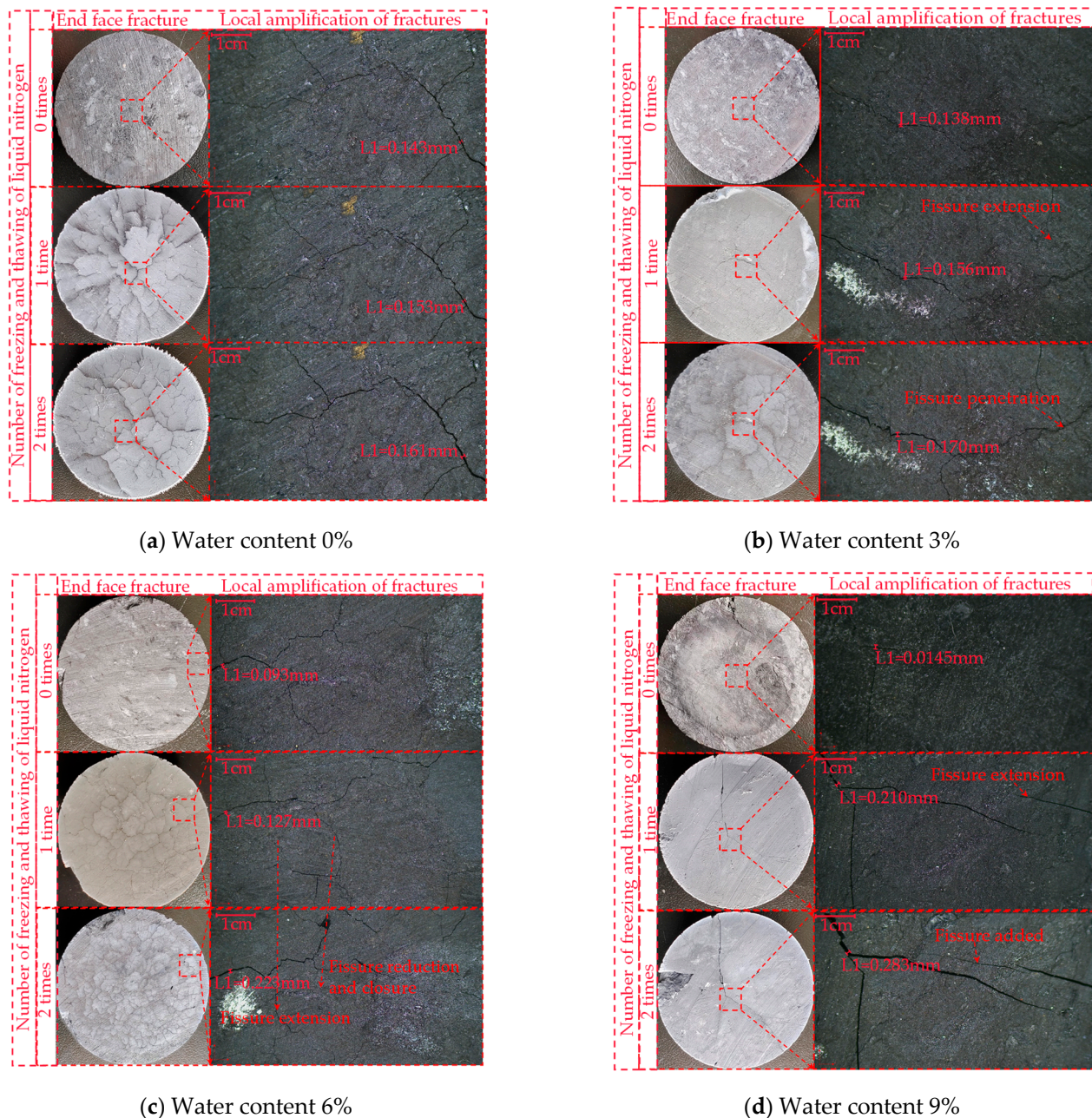


Figure 11. End face and local enlarged fracture after freeze–thawing of liquid nitrogen for specimens with different water content values.

6. Discussion

Most of the existing studies on low-temperature fracturing of coal bodies by liquid nitrogen have investigated the freezing time and cyclic freezing of coal bodies by liquid nitrogen, i.e., they mainly focus on the “freezing” aspect, but few studies have investigated the ablation time of coal bodies after freezing by liquid nitrogen, i.e., they lack the “melting” aspect [31–41]. Jia Peng [42] tested the elastic modulus and hardness of coal samples frozen by liquid nitrogen using the nanoindentation technique and concluded that the elastic modulus and hardness of coal samples increased after freezing by liquid nitrogen. Peng concluded that the reason was that the water in the pores and fissures of coal samples changed from liquid to solid after freezing, which supported the pores and fissures and thus increased the hardness.

In this paper, the freeze–thaw time of liquid nitrogen on media was 10 min of liquid nitrogen immersion and then natural thawing at room temperature for 2 h, which is consistent with most of the above-mentioned scholars' research. The coal rock strength was reduced after freeze–thawing of liquid nitrogen, but the actual downhole coal seam liquid nitrogen penetration needs to take into account the extraction plan, that is, to consider how long the gas extraction volume rises significantly after liquid nitrogen penetration, and to plan the extraction attainment time according to the gas extraction volume to arrange the subsequent production plan. Therefore, in follow-up research of liquid nitrogen low-temperature fracturing coal bodies, it is necessary to explore the perfect “melting” link, i.e., to study the effect of melting time on coal mechanics and seepage characteristics after the coal body is frozen by liquid nitrogen, to explore the effect of slow melting at room temperature and rapid melting by microwave radiation heat injection on the coal rock structure. The goal is to find a new method to achieve a rapid permeability increase in low-permeability coal rocks downhole.

7. Conclusions

As the global economy continues to develop rapidly, the need for various energy sources is increasing, and some conventional energy sources are no longer able to meet the growing needs of people. Therefore, this paper is designed to use liquid nitrogen cycle freeze–thaw to increase the permeability of coal rocks, through liquid nitrogen freeze–thaw pretreatment, and compare and analyze the effect of liquid nitrogen on the mechanics and seepage of coal rocks with different water content, in order to explore new methods of developing unconventional resources such as coalbed methane and shale gas, which will be of great importance to the sustainable development of global energy, and the following conclusions are mainly drawn:

- (1) Freeze–thawing of liquid nitrogen has a significant effect on the mechanical properties of water-bearing coal rocks. Under the treatment of freeze–thawing without liquid nitrogen, the peak strength and modulus of elasticity of coal samples showed a nonlinear decreasing trend. Poisson's ratio and axial peak strain showed nonlinear increasing trends with the increase in water content; after the treatment of freeze–thawing with liquid nitrogen, the peak strength and axial peak strain of coal samples showed a nonlinear decreasing trend, the modulus of elasticity showed an increasing trend and then a decreasing trend, and Poisson's ratio showed an increasing trend with the increase in water content. Compared with the non-freeze–thawed coal samples, the internal structural damage of coal rock after freeze–thawing by liquid nitrogen was obvious, which showed that the peak strength of liquid nitrogen freeze–thawed coal samples was smaller than that of non-freeze–thawed coal samples, and Poisson's ratio was larger than that of non-freeze–thawed coal samples at the same water content;
- (2) The local stress concentration of water-bearing coal rocks is significantly enhanced at each stage after the freeze–thawing of liquid nitrogen. Compared with the non-freeze–thawed coal samples, the strain fluctuations and concentrations in the stages of compression, flexibility, yielding, and damage of coal rocks after freeze–thawing with liquid nitrogen showed an overall weakening trend, but the local stress concentrations were more obvious. After the water-bearing coal sample was treated with liquid nitrogen freeze–thawing, the primary fracture extension and new fracture generation formed a fracture network, and the coal rock structure within the fracture network was more severely damaged than the coal rock structure around other fractures. The stress concentration was generated at the intersection point with the largest number of fracture branches in the fracture network when subjected to external load, and it was much more obvious than the stress concentration at the end point of new–old fractures, which led to the local stress concentration in each stage of coal rock after liquid nitrogen freeze–thaw. The stress concentration at each stage after freeze–thawing by liquid nitrogen was significantly enhanced;

- (3) The coal samples under conventional triaxial loading were mainly damaged by shear strain after freeze–thaw treatment with water and liquid nitrogen. The coal samples without liquid nitrogen freeze–thawing mainly showed single shear damage, and the damage fissures were mainly inclined fissures with small openings; the damage fissures of the coal samples with liquid nitrogen freeze–thawing were mainly inclined fissures with small openings, and the damaged specimens were a combination of blocks and powder; the coal samples with 3% and 6% water content values showed conjugate damage, and the damage fissures were mainly inclined fissures with large openings; the coal samples with 9% water content showed tension shear damage, and the damage fissures were mainly inclined fissures and circumferential fissures with large openings. Inclined fissures and circumferential fissures with large openings were the main ones;
- (4) The effect of liquid nitrogen freezing and thawing on the fracturing and permeability of water-bearing coal rocks is remarkable. With the increase in water content, the permeability of non-freeze–thawed coal samples showed a linear decreasing trend, and the permeability of coal samples was $0.03 \times 10^{-3} \mu\text{m}^2$ when the water content reached 9%, and there was basically no channel for gas circulation inside the coal samples; the permeability of frozen–thawed coal samples showed a non-linear increasing trend, and the higher the water content under the action of expansion force, the faster the permeability growth rate, and the permeability of coal samples could reach $6.30 \times 10^{-3} \mu\text{m}^2$ at 9% water content.

Author Contributions: S.H. and H.M. were responsible for the conception of experimental conditions and data analysis to write the manuscript; X.Q. was responsible for providing experimental funding, experimental guidance, and revision of the manuscript; P.W., Y.L. and X.W. were responsible for the experiments, data collection, and collation. All authors have read and agreed to the published version of the manuscript.

Funding: This research was funded by the Key Laboratory Open Fund Project of the Ministry of Education (Project No. JSK202010) and the National Natural Science Foundation of China (Project No. 52274205).

Institutional Review Board Statement: Not applicable.

Informed Consent Statement: Not applicable.

Data Availability Statement: The experimental data used to support the results of this study are available from the corresponding authors upon request.

Conflicts of Interest: The authors declare no conflict of interest.

References

1. Reng, S.H.; Xie, Y.H.; Jiao, X.M. Characteristics of carbon emissions during coal development and technical approaches for carbon neutral development. *Adv. Eng. Sci.* **2022**, *54*, 60–68.
2. Guo, X.B. Application of hydraulic punching hole-making technology in gas extraction. *Shandong Coal Sci. Technol.* **2018**, *15*, 69–70.
3. Weng, H.B. Research on Evaluation of Hydraulic Fracturing Effect and Prediction of Abatement Time of Coalbed Methane Wells. Master's Thesis, Henan University of Technology, Jiaozuo, China, 2015.
4. Zhang, C.H.; Wang, L.G.; Zhao, Q.S. Deformation–destruction–permeability evolution model and numerical analysis of liquid nitrogen-cooled coal. *J. Hebei Univ. Sci. Technol.* **2015**, *36*, 90–99.
5. Li, W.L. Experimental Study on the Fracturing and Permeability Enhancement of Coal by Liquid Nitrogen Soluble Leaching. Master Thesis, Hebei University of Science and Technology, Shijiazhuang, China, 2015.
6. Shia, J.Q.; Durucana, S.; Fujioka, M. A reservoir simulation study of CO₂ injection and N₂ flooding at the Ishikari coalfield CO₂ storage pilot project, Japan. *Int. J. Greenh. Gas Control* **2008**, *2*, 47–57. [[CrossRef](#)]
7. Settari, A.; Bachman, R.C.; Bothwell, P. Analysis of Nitrogen stimulation technique in shallow CBM formations. In Proceedings of the SPE Annual Technical Conference and Exhibition, Florence, Italy, 19–22 September 2010; p. SPE 135683.
8. Wang, S.K.; Zhang, W.B.; Pan, Q.L. Study on the effect of water on the impact tendency characteristics of coal. *Mine Press.* **1987**, *50*, 56+64.

9. Cheng, Q.W. Mechanism of Coal Rock Permeability Evolution under the Synergistic Effect of Intrinsic Water, Proppant and Effective Stress. Master's Thesis, Guizhou University, Guiyang, China, 2022.
10. Chang, Y.N. Analysis of Impact Propensity of Hard Coal Rocks with Different Water Content and Optimization of Water Injection Parameters in Anti-Inflammation Coal Seams. Master's Thesis, Inner Mongolia University of Science and Technology, Baotou, China, 2022.
11. Ren, S.R.; Fan, Z.K.; Zhang, L. Mechanism and experimental study of cold impact effect of liquid nitrogen on coal rock. *Chin. J. Rock Mech. Eng.* **2013**, *32*, 3790–3794.
12. Ren, Y.J.; Wei, J.P.; Li, B. Study on the fine damage characteristics of coal rocks under the effect of liquid nitrogen cold leaching. *J. Henan Univ. Sci. Technol. (Nat. Sci. Ed.)* **2022**, *41*, 18–25.
13. Wang, H. Mechanical Evolution and Numerical Simulation of Low Temperature Fractured Coal. Master's Thesis, Taiyuan University of Technology, Taiyuan, China, 2021.
14. Coetzee, S.; Neomagus, H.W.; Bunt, J.R.; Strydom, C.A.; Schobert, H.H. The transient swelling behaviour of large South African coal particles during low-temperature devolatilisation. *Fuel* **2014**, *136*, 79–88. [[CrossRef](#)]
15. Cai, C.Z.; Li, G.S.; Huang, Z.W. Experimental study of the effect of liquid nitrogen cooling on rock pore structure. *J. Nat. Gas Sci. Eng.* **2014**, *21*, 507–517. [[CrossRef](#)]
16. Li, B.; Ren, Y.J.; Zhang, L.L. Study on the mechanism of the effect of liquid nitrogen on the permeability enhancement of water-bearing coal rock bodies. *Coal Sci. Technol.* **2018**, *46*, 145–150.
17. Liu, G. Research on Triaxial Soil Sample Shear Damage Process Based on Full Surface Measurement. Master's Thesis, Dalian University of Technology, Dalian, China, 2017.
18. Dong, J.J. Study on Stress-Strain Characteristics of Unsaturated Compacted Soil Based on Digital Image Measurement. Master's Thesis, Dalian University of Technology, Dalian, China, 2008.
19. Liu, G.; Guo, X.X. Study on shear damage characteristics of layered specimens based on digital image measurement method. *Exp. Mech.* **2022**, *37*, 77–87.
20. Gao, J.C.; Guo, Y.; Jia, J.Q. Study on the progressive damage characteristics of saturated fine sand based on digital image measurement system. *Rock Soil Mech.* **2016**, *37*, 1343–1350.
21. Shao, L.T.; Guo, X.X.; Liu, G. Application of digital image measurement technology in geotechnical triaxial tests. *Rock Soil Mech.* **2015**, *36*, 669–684.
22. Dong, J.J.; Shao, L.T.; Liu, Y.L. Measurement of deformation of unsaturated compacted soil specimens in three axes based on image measurement method. *Rock Soil Mech.* **2008**, *150*, 1618–1622.
23. Griffith, A.A. The phenomena of rupture and flow in solids. *Philos. Trans. R. Soc. Lond. Ser. A* **1920**, *221*, 163–198.
24. Bobet, A.; Einstein, H.H. Fracture coalescence in rock-type materials under uniaxial and biaxial compression. *Int. J. Rock Mech. Min. Sci.* **1998**, *35*, 863–888. [[CrossRef](#)]
25. Yang, S.Q.; Huang, Y.H.; Tian, W.L. Effect of High Temperature on Deformation Failure Behavior of Granite Specimen Containing a Single Fissure Under Uniaxial Compression. *Rock Mech. Rock Eng.* **2019**, *52*, 2087–2107. [[CrossRef](#)]
26. Gan, H.; Nandi, S.; Walker, P., Jr. Nature of the porosity in American coals. *Fuel* **1972**, *51*, 272–277. [[CrossRef](#)]
27. Thommes, M.; Kaneko, K.; Neimark, A.V. Physisorption of gases, with special reference to the evaluation of surface area and pore size distribution (IUPAC Technical Report). *Pure Appl. Chem.* **2015**, *87*, 1051–1069. [[CrossRef](#)]
28. Ding, K.; Wang, L.; Wang, W.; Li, Z.; Jiang, C.; Ren, B.; Wang, S. Experimental Study on Gas Seepage Characteristics of Axially Unloaded Coal under Different Confining Pressures and Gas Pressures. *Processes* **2022**, *10*, 1055. [[CrossRef](#)]
29. Li, Q.; Liang, Y.; Zou, Q. Seepage and Damage Evolution Characteristics of Gas-Bearing Coal under Different Cyclic Loading–Unloading Stress Paths. *Processes* **2018**, *6*, 190. [[CrossRef](#)]
30. Winkler, E.M. Frost damage to stone and concrete: Geological considerations. *Eng. Geol.* **1968**, *2*, 315–323. [[CrossRef](#)]
31. Yang, R.; Cong, R.; Liu, H. Pore-scale analysis of coal structure and mechanical properties evolution through liquid nitrogen thermal shock. *Nat. Gas Ind. B* **2021**, *8*, 596–606. [[CrossRef](#)]
32. Chen, S.; Zhang, L.; Zhang, C. Experimental study on the seepage characteristics of bituminous coal under the conditions of liquid nitrogen fracturing. *Energy Sci. Eng.* **2019**, *7*, 2138–2154. [[CrossRef](#)]
33. Akhondzadeh, H.; Keshavarz, A.; Awan, F.U.R. Coal fracturing through liquid nitrogen treatment: A micro computed tomography study. *APPEA J.* **2020**, *60*, 67–76. [[CrossRef](#)]
34. Zhang, L.; Chen, S.; Zhang, C. The characterization of bituminous coal microstructure and permeability by liquid nitrogen fracturing based on μ CT technology. *Fuel* **2020**, *262*, 116635. [[CrossRef](#)]
35. Akhondzadeh, H.; Keshavarz, A.; Awan, F.U.R. Liquid nitrogen fracturing efficiency as a function of coal rank: A multi-scale tomographic study. *J. Nat. Gas Sci. Eng.* **2021**, *95*, 104177. [[CrossRef](#)]
36. Ali, M.; Shar, A.M.; Mahesar, A.A. Experimental evaluation of liquid nitrogen fracturing on the development of tight gas carbonate rocks in the Lower Indus Basin, Pakistan. *Fuel* **2022**, *309*, 122192. [[CrossRef](#)]
37. Yang, R.; Hong, C.; Huang, Z. Liquid nitrogen fracturing in boreholes under true triaxial stresses: Laboratory investigation on fractures initiation and morphology. *SPE J.* **2021**, *26*, 135–154. [[CrossRef](#)]
38. Wu, Y.; Tao, J.; Wang, J. Experimental investigation of shale breakdown pressure under liquid nitrogen pre-conditioning before nitrogen fracturing. *Int. J. Min. Sci. Technol.* **2021**, *31*, 611–620. [[CrossRef](#)]

39. Huang, C.W.; Bit Jiang, W.; Li, G.S. Experimental study on the effect of liquid nitrogen freezing on the tensile and compressive strength of rocks. *Geotech. Mech.* **2016**, *37*, 694–700+834.
40. Cai, C.; Tao, Z.; Ren, K. Experimental investigation on the breakdown behaviours of sandstone due to liquid nitrogen fracturing. *J. Pet. Sci. Eng.* **2021**, *200*, 108386. [[CrossRef](#)]
41. Wen, H.; Yang, R.; Huang, Z. Flow and heat transfer of nitrogen during liquid nitrogen fracturing in coalbed methane reservoirs. *J. Pet. Sci. Eng.* **2022**, *209*, 109900. [[CrossRef](#)]
42. Jia, P. Quantitative Characterization and Change Mechanism of Microscopic Pore Structure and Mechanical Properties of Liquid Nitrogen Frozen Coal Body. Master's Thesis, Liaoning University of Engineering and Technology, Fuxin, China, 2022.

Disclaimer/Publisher's Note: The statements, opinions and data contained in all publications are solely those of the individual author(s) and contributor(s) and not of MDPI and/or the editor(s). MDPI and/or the editor(s) disclaim responsibility for any injury to people or property resulting from any ideas, methods, instructions or products referred to in the content.